RSC Advances

ROYAL SOCIETY
OF **CHEMISTRY**

www.rsc.org/advances

RSC Advances

ARTICLE

Back to basics: Identification of reaction intermediates in the mechanism of a classic ligand substitution reaction on Vaska's complex

Clara J. Durango-García[a,b] Said Jalife,[c] José Luis Cabellos,[c] Saul H. Martínez,[c] J. Oscar C. Jimenez-Halla,[d] Sudip Pan,[e] Gabriel Merino,[c*] and Virginia Montiel-Palma[a*]

The mechanism of methylation of Vaska's complex trans-[ClIr(CO)(PPh$_3$)$_2$] by trimethylgallium was studied and the identification of the spectroscopically detected intermediates was achieved with the aid of computational methods. The reaction pathway, computed by means of density functional theory (M05-2X-D3/def2-SVP), involves the initial formation of chloride-bridged adduct trans-[(ClGaMe$_3$)Ir(CO)(PPh$_3$)$_2$] to then proceed to a transition state [(μ_2-Cl,C-ClMeGaMe$_2$)Ir(CO)(PPh$_3$)$_2$]. This transition state subsequently evolves to the methylated adduct [MeIr(CO)(PPh$_3$)$_2$·(GaMe$_2$Cl)] to finally release the alkylated product trans-[MeIr(CO)(PPh$_3$)$_2$] together with GaMe$_2$Cl.

Introduction

Understanding about the bonding nature and properties of compounds containing transition metals directly bound to a group 13 element is important partly because of their potential use as catalysts and in material science applications.[1] In our search for synthetic methods leading to the formation of such compounds, we have reported the reaction between IrHCl$_2$(PCy$_3$)$_2$ and GaMe$_3$ (1:3 molar ratio), which proceeds cleanly to the formation of the gallyl compound (GaMe$_3$·Cl)IrMe(GaMe$_2$)(PCy$_3$)$_2$ (Eq. 1).[2] Under similar conditions, the analogous reaction of Vaska's complex trans-[ClIr(CO)(PPh$_3$)$_2$] (1) with excess GaMe$_3$ proceeds only to the alkyl derivative trans-[(CO)IrMe(PPh$_3$)$_2$,][3] (2) (Eq. 2), and GaMe$_2$Cl with no evidence of heterobimetallic products. Since complex 1 and its analogues are amongst the preferred organometallic species for reaction mechanism studies,[4-11] we decided to investigate this reaction focusing on the detection of possible reaction intermediates in the form of adducts containing gallium or heterobimetallic intermediates.

(Eq. 1)

(Eq. 2)
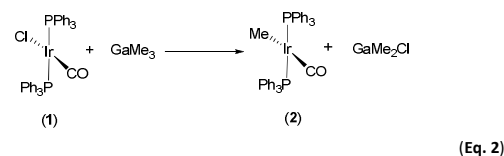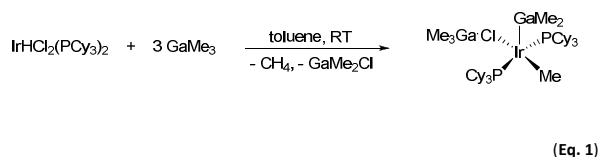
The reported experimental investigations on ligand substitution reactions on complex 1 have mainly concentrated on the kinetics and associative and exchange mechanisms have been proposed for ligand substitutions.[12] From a strict point of view, the elucidation of reaction mechanisms needs not only a good knowledge of the kinetics, which often gives valuable information, but also of the properties of the intermediates involved. In other words, how the reaction rate varies with the concentration of reactants, temperature, and other conditions gives vital clues but rarely establishes with certainty the mechanism of the process.[13] Photochemical studies aside,[14-18] to our knowledge, only relatively few efforts have addressed the determination of reaction intermediates stemming from Vaska's related compounds in thermal processes.[19,20] Herein we use density functional theory (DFT) to assign the identity of the intermediates for the ligand substitution reaction of chloride by methyl in 1 which indeed proceeds via an associative mechanism involving a chloride-bridged transition state.

a. Centro de Investigaciones Químicas, Universidad Autónoma del Estado de Morelos, Av. Universidad 1001, Col. Chamilpa, Cuernavaca, Morelos, C. P. 62209, México. E-mail: vmontielp@uaem.mx
b. Facultad de Ciencias, Universidad Antonio Nariño sede Armenia, Av. Bolívar # 49 Norte 30. Armenia, Quindío, Colombia.
c. Departamento de Física Aplicada, CINVESTAV Unidad Mérida, km. 6, Antigua Carretera a Progreso, AP 73, Cordemex, Mérida 97310, Yucatán, México. E-mail: gmerino
d. Departamento de Química (DCNE), Universidad de Guanajuato, Noria Alta s/n, 36050, Guanajuato, México.
e. Department of Chemistry and Center for Theoretical Studies, Indian Institute of Technology Kharagpur, 721302, India.

Materials and Methods

General experimental procedures

All experiments were performed under argon atmosphere inside an MBraun glove box. Deuterated benzene was dried over molecular sieves and degassed via three freeze-pump-thaw cycles. Compound **1**[21] and authentic compound **2** were synthesized for comparison according to the reported procedures.[3,22] NMR spectra were recorded on a Varian Inova 400 MHz in NMR tubes fitted with J. Young's valves and using 0.5 mL solvent volume. IR spectra were collected on a Nicolet FTIR 6700 series spectrophotometer.

Computational Details

All geometries were fully optimized using the M05-2X[23] functional in conjunction with a def2-SVP basis set employing Gaussian 09 program package.[24] In order to incorporate dispersion, Grimme´s D3 dispersion scheme[25] was included during the optimization. The nature of stationary points located on the potential energy surface (PES) was characterized by harmonic vibrational frequency analysis. Thermal corrections were computed within the harmonic approximation. An intrinsic reaction coordinate (IRC) calculation was done in order to verify that the transition state was truly connected to the correct minima. Solvation energy corrections for benzene were evaluated by a self-consistent reaction field (SCRF) using the Solvation Model based on Density (SMD)[26] model under the same level. All calculations were done using an ultrafine integration grid.

In order to evaluate the thermal effects, we used the procedure described by Irikura as is implemented in thermo code,[27] where the estimation of the standard molar entropy and enthalpy change is computed from the molecular partition function. All the quantities needed are taken from the harmonic vibrational frequency computations.

The nature of the interactions was analyzed by energy decomposition analysis (EDA)[28] at the PBE-D3/DZP//M05-2X-D3/def2-SVP level using the ADF (2013.01) package[29] (TZVP basis set is used for Ir). Frozen core approximation was not used here. Scalar relativistic effects were considered using the zeroth-order regular approximation (ZORA).[30] In EDA, bond formation between the interacting fragments can be represented by the following three successive steps. Firstly, the fragments, which are calculated with the frozen geometry of the entire molecule, are superimposed without electronic relaxation. It yields the quasiclassical electrostatic attraction (ΔE_{elstat}). Secondly, the product wave function becomes antisymmetrized and renormalized providing the Pauli repulsion term (ΔE_{Pauli}). In the next step the molecular orbitals undergo relaxation to go into their final form yielding the stabilizing orbital interaction (ΔE_{orb}). Since we used dispersion corrected PBE-D3 functional, the dispersion correction term

(ΔE_{disp}) will be added to the interaction energy (ΔE_{int}) values to describe the total bond energy as

$$\Delta E_{int} = \Delta E_{Pauli} + \Delta E_{elstat} + \Delta E_{orb} + \Delta E_{disp} \qquad \text{(Eq. 3)}$$

The ΔE_{int} is related to the bond dissociation energy, D_e, by adding ΔE_{prep}, which is the necessary energy needed to promote the fragments from their equilibrium geometry to the geometry in the complexes (Eq 4). The advantage of using ΔE_{int} instead of D_e is that the instantaneous electronic interaction of the fragments becomes analyzed, which yields a direct estimate of the energy components.

$$-D_e = \Delta E_{prep} + \Delta E_{int} \qquad \text{(Eq. 4)}$$

Results and Discussion

Spectroscopic evidence

The reactions between **1** and $GaMe_3$ in different stoichiometric ratios were monitored by NMR and IR spectroscopies. For spectroscopic studies, the addition of the organogallium was made upon frozen mixtures of **1** in 0.5 mL benzene-d_6 and the spectra recorded as soon as possible after thawing. At the molar ratio 0.5:1 (corresponding to $GaMe_3$:**1**), the NMR data were in agreement with partial formation of the methylated product **2**.[22,§] In addition, the ^{1}H NMR spectrum recorded at 280 K shows two singlet signals of small intensity at $\delta = 0.22$ and 0.08 ppm. The former signal is assigned to the generated $GaMe_2Cl$ whilst the latter to intermediate species **I1** (Table 2). Due to the low concentration of **I1** and the fact that this species does not persist in solution for longer than 5 min at 280 K, it was not possible to record its ^{31}P NMR spectrum. A sample prepared under identical conditions (benzene-d_6) was studied by IR spectroscopy in solution showing an additional carbonyl stretching band at 1965 cm^{-1}, which is detectable only at short (< 5 min) reaction times and we thus attributed it also to species **I1** (Table 2). The NMR tube containing the reaction mixture $GaMe_3$:**1** (0.5:1 molar ratio) was allowed to warm up to 298 K during 5 min after mixing and the ^{1}H NMR spectrum was recorded again. It showed evidence for the exchange of free and coordinated $GaMe_3$ in the alkyl region as the signal due to the latter (at $\delta = 0.15$ ppm at 280 K) and the new small signal at $\delta = 0.08$ ppm merge into a broad signal in the region of $-0.04 < \delta < 0.75$ ppm. The reaction of $GaMe_3$ and **1** in a 1:1 molar ratio was performed under the same conditions and the ^{1}H NMR spectrum collected immediately afterwards showed near-to-complete conversion of **1** to **2**, as well as a new signal of small intensity at $\delta = 0.38$ (t), which persists for few minutes later fully evolving to **2**. Once again, rapid transformation to products and low concentration of the possible intermediate species prevented the acquisition of the ^{31}P NMR spectrum. An independently but identically prepared sample for IR spectroscopy showed the presence of a new band at 1970 cm^{-1} (Table 2).

After comparison with reported frequencies of other adducts of **1**,[20c,21,31,32] we propose that these experimental findings can

be understood if a first intermediate species, **I1,** is formed at lower concentrations of GaMe$_3$, which incorporates at least one intact molecule of GaMe$_3$ such as to be able to exchange it with free GaMe$_3$ present in the reaction medium. The carbonyl band at 1965 cm^{-1} in the IR spectrum and the ^{1}H signal at $\delta =$ 0.08 ppm would be then due to **I1**. Addition of further organogallium (ratio 1:1 or higher) results in the formation of **2**, together with species, **I2**, observed by IR at 1970 cm^{-1} and in the ^{1}H NMR at $\delta =$ 0.38 ppm as a triplet. The formation of GaMe$_2$Cl was spectroscopically ascertained by ^{1}H and ^{13}C NMR spectra.

Investigation of the Reaction Mechanism by DFT

Since it was not possible by experimental means to ascertain the identity of the intermediate species, we turned to computational methods to gain insights into their structure. The electrostatic potential of **1**, plotted in Figure 1, clearly shows the presence of negative regions around Cl, O and Ir, indicating that these sites are susceptible for an electrophilic attack. According to the NBO charges, Ir exhibits a charge of -0.70 |e|, followed by O (-0.49 |e|) and Cl (-0.43 |e|). So, compound **1** (Figure 1) has three probable sites to coordinate a with GaMe$_3$ unit. In Figure 2, these options are depicted: in (**A**) the gallium coordinates through the chlorine atom, in (**B**) via the oxygen atom of the carbonyl group, and in (**C**) through the iridium itself.
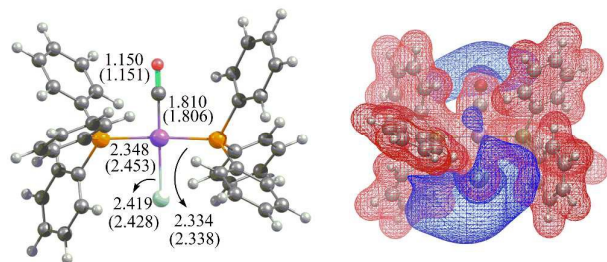

Figure 1. M05-2X-D3/def2-SVP geometry of **1** and its electrostatic potential surface. Blue (-0.03 a.u) and red (0.05 a.u.) regions represent negative and positive electrostatic potentials, respectively. Selected bond distances are shown in Å, in parenthesis the corresponding distances found upon inclusion of solvent. Atom colour code: C (black), Cl (light blue), H (grey), Ir (purple), O (red), P (orange).

Our M05-2X-D3/def2-SVP computations indicate that **A** is the lowest-lying energy structure. **B** and **C** are higher in energy than **A** by 4.1 and 0.5 kcal·mol^{-1}, respectively. At 280 K (the temperature employed to record the ^{1}H NMR spectrum), the thermal effects change moderately the above energy differences (ΔG^{280K}_{A-B} = 3.0 kcal/mol and ΔG^{280K}_{A-C} = 2.8 kcal/mol). Similar results are obtained using other functionals when dispersion is included (Table S1). On the other hand, assuming a scale factor of 0.914 (details in the supporting information), the calculated frequencies for the CO stretching vibrations are 1964 (**A**), 1864 (**B**), and 1970 cm^{-1} (**C**). The experimental value for **I1** is 1965 cm^{-1} (Table 2). In principle,

the chlorine-bridged adduct *trans*-[(Me$_3$Ga$^-$Cl)Ir(CO)(PPh$_3$)$_2$] is the best candidate for **I1**.

The temperature significantly affects the bond dissociation energies (BDE) of the three complexes. The computed dissociation energies at 0 K, including the ZPE corrections, are 20.4 (**A**), 16.3 (**B**), and 19.9 (**C**) kcal·mol^{-1}. At 280 K, the calculated BDE values are 6.0 (**A**), 3.0 (**B**), and 3.2 (**C**) kcal·mol^{-1}. Figure 3 shows the variation of the free energy differences with temperature. It indicates that while **A** is stable until 470 K, **B** and **C** are stable complexes until only 320 K. Populations of each species estimated via Boltzmann distributions suggest that at 280 K and 1 atm, structures **B** and **C** contribute with less than 1%.
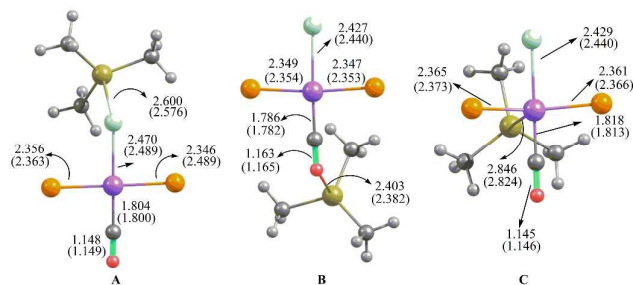

Figure 2. Three modes of coordination of GaMe$_3$ to Vaska's complex, **1**, computed at the M05-2X-D3/def2-SVP level. Selected bond distances are shown in Å, in parentheses the corresponding distances found upon inclusion of solvent. Atom colour code: C (black), Cl (light blue), Ga (olive green), H (grey), Ir (purple), O (red), P (orange).

To gain a quantitative insight into the nature of the bonding interactions in these complexes, we also perform an EDA, using GaMe$_3$ and Vaska's complex as interacting fragments for **I1**, **B**, and **C**, and GaMe$_2$Cl with alkyl derivative of Vaska's complex for **I2**. Clearly, the principal factor to stabilize the three possible reactant complexes and even the product complex is electrostatic (around 46.5±4.0%, Table 1). The orbital term contributes with around 37.0±3.0%. The most important differences among the complexes come from the dispersion term. The dispersion term in complex **B** is much significant than in complexes **A** and **C**. It is well known that interactions with a high noncovalent nature are more affected by the temperature. In our cases, though in all of the complexes the dispersion is important, but **B** will be more affected by the temperature.

Note the large difference between the BDEs and the ΔE_{int} values. It denotes strong structural changes of the reactants during the formation of the complexes. Our computations show that the structural changes in the GaMe$_3$ fragment are the most energetically expensive. In other words, the deformation of the Lewis acid not only influences dissociation energies, but also changes the electron distribution of the acid as it triggers changes in the gallium hybridization.

Table 1. EDA results of the coordination of GaMe$_3$ to Vaska complex studied at the PBE-D3/DZP//M05-2X-D3/def2-SVP level. Energies are in kcal/mol.

Complex	ΔE_{elstat}	ΔE_{Pauli}	ΔE_{orb}	ΔE_{disp}	ΔE_{int}
I1	-28.5 (45.3)	37.6	-23.5 (37.4)	-10.9 (17.3)	-25.3
Complex B	-18.2 (43.1)	23.9	-14.3 (33.9)	-9.7 (23.0)	-18.3
Complex C	-40.1 (46.7)	51.9	-32.1 (37.4)	-13.6 (15.9)	-34.0
I2	-73.5 (50.8)	93.3	-58.2 (40.2)	-13.0 (9.0)	-51.4

Table 2. Experimental carbonyl group stretching frequencies in cm^{-1} (in parenthesis computed values) and ^{1}H NMR shifts in the alkyl region in ppm for the species involved.

Species	ν(CO)	^{1}H NMR shifts (alkyl region)	Assignment
1	1951[a]	–	*trans*-[ClIr(CO)(PPh$_3$)$_2$]
I1	1965[b] (1964)	0.08 (s)	*trans*-[(GaMe$_3$Cl)Ir(CO)(PPh$_3$)$_2$]
I2	1970[b] (1984)	0.38 (t, $^2J_{HP}$ 8.8 Hz)	[MeIr(CO)(PPh$_3$)$_2$·(GaMe$_2$Cl)]
2	1935[b]	0.48 ppm (t, $^2J_{HP}$ 9 Hz)	*trans*-[MeIr(CO)(PPh$_3$)$_2$]

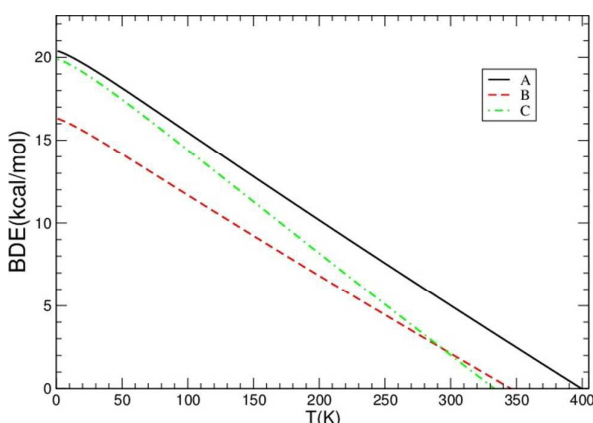[a] KBr disc. [b] C$_6$D$_6$ solution.

Figure 3. Bonding dissociation energies at different reaction temperatures for the three possible adducts of GaMe$_3$-Vaska's complex shown in Figure 1.

I1 shows an almost undistorted Ir center in a square planar geometry in which the Ir-Cl bond length has been very slightly elongated (2.470 Å) with respect to the corresponding distance in the calculated unreacted species **1** at 2.419 Å (Figure 1). The Cl¨Ga distance at 2.600 Å is still longer than that reported for covalent Ga-Cl bonds (*ca.* 2.23 Å) [33,34] but it is close enough to establish a bonding interaction. This is presumably due to the fact that between the solid state structure and that in the gas phase for a dative bond the variations could be higher than 0.1 Å. [35,36] In the extreme cases, these differences could be even higher than 0.8 Å. The Ir-Cl-Ga bond angle of 123.2° for the adduct **I1** is considerably more acute than that in reported (GaMe$_3$Cl)IrMe(GaMe$_2$)(PCy$_3$)$_2$ (168.86° and 161.05°)[2], nonetheless other group 13 adducts exhibit rather small Ir-Cl-E (E = Tl, B) angles. [37,38]

Figure 4 depicts the transition state involved in the transformation from **I1** to [MeIr(CO)(PPh$_3$)$_2$·(GaMe$_2$Cl)] (**I2**). The relative energy between **I1** and the transition state at 0 K is 16.0 kcal·mol^{-1}. This barrier slightly increases at 280 K (18.9 kcal·mol^{-1}).

The reaction proceeds via a transition state **TS** of a distorted trigonal bipyramid geometry, namely μ$_2$-methylchloro [(μ$_2$-*Cl,C*-ClMeGaMe$_2$)Ir(CO)(PPh$_3$)$_2$], with the two phosphines in the axial positions. The Cl atom bends away from the original square planar disposition in **1** and **I1**. In **TS**, the Cl is forming part of the equatorial base together with CO and one of the methyl groups of the GaMe$_3$ fragment. The angles around Ir in the equatorial plane are 80.3°, 130.0° and 148.4° largely deviated from the ideal 120° and arising from the approach of the methyl group to the Ir. In fact, while the Ir-Cl bond distance has further elongated to 2.760 Å, the Ir-C bond at 2.706 Å is short enough to be considered of importance. On the other hand, the Ga atom is only slightly deviated from the equatorial plane but exhibits a long non-bonding Ga¨Ir separation of 3.396 Å.
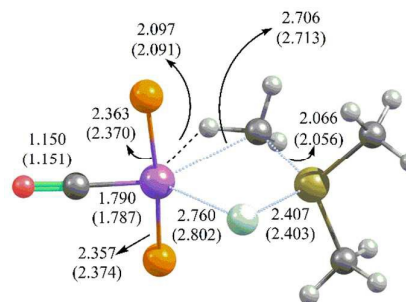

Figure 4. M05-2X-D3/def2-SVP geometry of the transition state involved in the methylation of Vaska's complex. Representative bond lengths (in Å) are shown, in parenthesis the corresponding lengths found upon inclusion of solvent. Atom colour code: C (black), Cl (light blue), Ga (olive green), H (grey), Ir (purple), O (red), P (orange).

Further geometrical analysis of **TS** reveals a short calculated Ir-H distance of 2.097 Å between one of the hydrogens of the methyl group and the metal centre. This distance is short enough to consider it of agostic type. The agostic H-C-Ir bond angle (46.3°) is considerably smaller than those of the corresponding angles for the non-agostic hydrogens on the same carbon atom (120.5° and 125.8°). Other geometrical parameters such as the Ir-H-C angle of 111.0° and the H-C-Ga angle at 135.8° are well within reported values of systems for which an agostic interaction is established. [39]

Evolution of the reaction leads to the formation of **I2** (see Figure S1) in which the methylated product has formed but which bears a $GaClMe_2$ fragment coordinated to Ir in the apical position of a square pyramid. At 0 K, **I2** is more stable than **I1** by 3.3 kcal·mol^{-1}. However, at 280 K the free energy difference is negligible, but the transformation from **I1** to **I2** is still exergonic (ΔG^{280K}_{I1-I2} = -0.7 kcal·mol^{-1}). No agostic C-H···Ir interactions are established here and the structural parameters are rather close to the isolated final product. The computed Ir…Ga distance in **I2** of 2.607 Å is still larger than the only other three X-ray structures reported to date, bearing direct Ir-Ga bonds, namely $[MeIr(PCy_3)_2(GaMe_2)(Cl^-GaMe_3)]$,[2] which has an Ir-Ga bond of 2.381(1)–2.389(2) Å, $[Ir(GaMe_2)CMe=CH_2\{N(SiMe_2-CH_2PPh_2)_2\}]$ of 2.411(2) Å,[40] and $Ir(1,5-COD)(IMes)\{Ga\{[N(Ar)C(H)]_2\}\}$ (where IMes = $:C\{N(C_6H_2Me_3-2,4,6)CH\}_2$) of 2.448(7) Å.[41] Note that the Ir…Ga length of **I2** is however shorter than that of complex **C** (2.846 Å), indicating a weak heterobimetallic interaction. Our computations show that the dissociation **I2** into **2** (Figure S2) and $GaMe_2Cl$ (12.9 kcal/mol) is two times higher than that of **I1** (6.0 kcal/mol); so **I2** is considerably more stable than **I1**. The computed frequency for the CO stretching vibration of **I2** is 1984 cm^{-1}, which is in good agreement with the experimental value of 1970 cm^{-1} (Table 2).
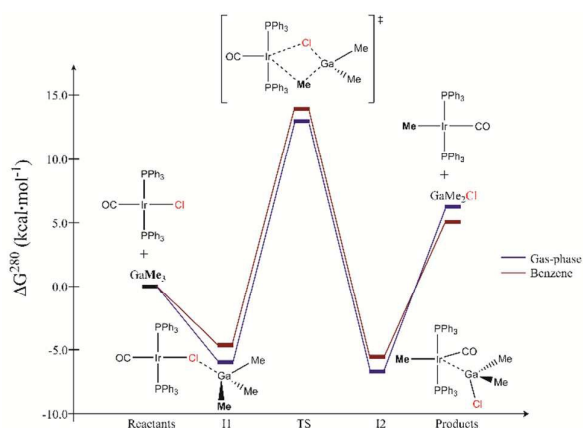

Figure 5. The Gibbs energy free profile computed at the M05-2X-D3/def2-SVP level at 280 K. In red is the profile including benzene as solvent. All values are in kcal/mol.

The computed mechanism is in agreement with other reports on ligand replacement or addition in low-valent transition metal complexes,[42] aside from the proposed agostic interaction precluding the formation of the Ir-Me bond. However, this type of interaction has been well identified by others when counting for the stabilization of reaction intermediates or transient species[43] in a variety of reaction mechanisms. Macgregor's work on the stability of *trans*-$(CO)Ir(XMe)(PPh_3)_2$ (X = O, CH_2) is particularly relevant as agostic interactions are proposed to account for the transformation between subsequent transition states.[44] To this point the overall transformation from **1** into **2** is still somewhat unclear because the ΔG^{280K}_{1-2} is 6.2 kcal/mol.

Additionally, the structures of **TS, I1** and **I2**, all possess large dipole moments (in the range of 5.2 to 7.7 D), and thus the geometries in the gas phase may be quite different from those in solution. However, since the reaction is performed using benzene as solvent we do not expect significant variations in the geometries and the energy profiles as a consequence of solvent effects (see ESI). This latter point is evident from Figures 1 and 2 in which the geometries do not show substantial changes when solvent is included in the computations. The largest variation is found in **TS** where the Ir-Cl bond distance changes by 0.04 Å. Moreover, Figure 5 shows the free energy profiles for the reaction with and without solvent effects. It can be seen that inclusion of the solvent does not alter significantly the energy differences and most importantly the overall reaction is still endergonic. So, how to explain the formation of free compound **2**?

Certainly, one possibility of a coupled reaction is the formation of gallium dimers. At the M05-2X-D3/def2-SVP level, the dimerization energy of $GaMe_3$ at 280K is endergonic (4.3 kcal/mol) in the gas phase. A similar value is obtained in solution (4.0 kcal/mol). In contrast, the dimerization energy of $GaMe_2Cl$ is −24.0 kcal/mol in the gas phase at 280 K and −18.0 kcal/mol in solution at the same temperature. These values suggest that dimerization of $GaMe_2Cl$ is the driving force for the conversion of **1** to **2**. These results are in agreement with the reported structures of organogallium compounds both in solid state and in the gas phase. Indeed, in contrast to the monomeric nature of $GaMe_3$,[45] gallium chlorides Me_xGaCl_{3-x} (x =0, 1, 2) exhibit dimeric structures with a central Ga_2Cl_2 core.[46] Our findings suggest that the aggregation of $GaCl_2Me$ as a dimer is crucial for the alkylation reaction from $GaMe_3$.

Conclusions

The use of $GaMe_3$ instead of more powerful alkylating ligands such as Li or Mg derivatives allows the spectroscopic detection of reaction intermediates under controlled conditions. The computational work has contributed to the assignment of the observed intermediate species **I1** as *trans*-[(Cl $GaMe_3$)Ir(CO)(PPh_3)_2] and **I2** as $[MeIr(CO)(PPh_3)_2·(GaMe_2Cl)]$. The transition state **TS**, comprising the two metal moieties in a metathesis-like reaction, is stabilized by an agostic C-H bond interaction. Although it is a simple ligand replacement reaction on a 16-electron Ir(I) complex, the present mechanism of alkylation of Vaska´s compound (**1**) by $GaMe_3$ is in agreement with previous work highlighting the importance of the halide substituent on the reaction and the agostic interactions for the stabilisation of the transition state. In this case, a Cl$^-$GaMe$_3$ adduct formation precedes the transition state. Finally, species **TS** and **I2** both show weak interacting heterobimetallic Ir-Ga bonds.
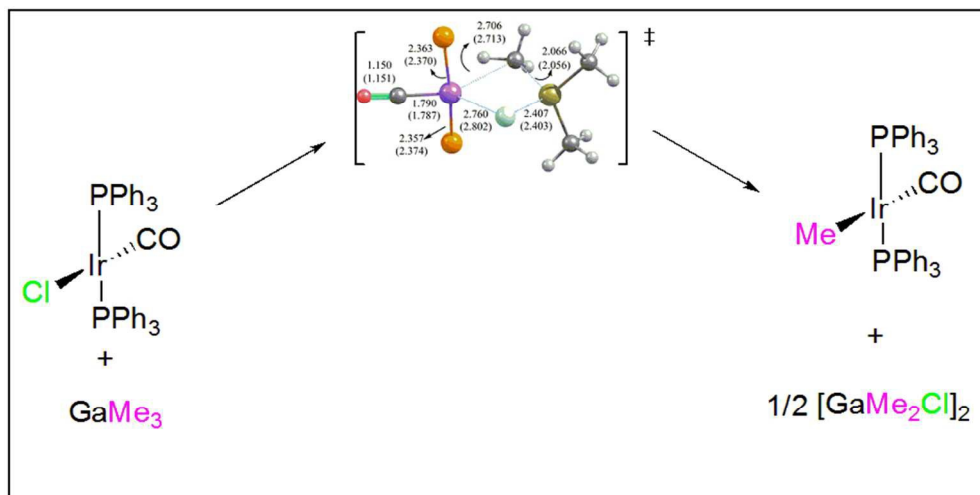
Acknowledgements

Notes and references

§ The formation of **2** was previously known to occur from excess MeLi addition to **1** followed by addition of magnesium silicate, however no further details were provided for that transformation. Reference 3.

§§ The main spectroscopic features of an authentic sample of **2** prepared as reported in reference 3 are a triplet at δ 0.48 ppm ($^2J_{HP}$ = 9Hz) in the ^{1}H NMR, a singlet at 31.9 ppm in the ^{31}P{^{1}H} NMR in C_6D_6 and a carbonyl stretching band at 1935 cm^{-1}.

1   (a) R. A. Fischer and J. Weiβ, *Angew. Chem., Int. Ed.,* 1999, **38**, 2830; (b) A. H. Cowley and R. A. Jones, *Angew. Chem. Int. Ed. Engl.*, 1989, **28**, 1208; (c) M. L. Hitchman and K. F. Jensen, *Chemical Vapor Deposition,* Academic Press, London, 1993; (d) H. Braunschweig, K. Gruss and K. Radacki, *Angew. Chem., Int. Ed.,* 2007, **46**, 7782.

2   C. J. Durango-García, J. O. C. Jiménez-Halla, M. López-Cardoso, V. Montiel-Palma, M. A. Muñoz-Hernández and G. Merino, *Dalton Trans.*, 2010, 10588.

3   W. M. Rees, M. R. Churchill, Y. J. Li and J. D. Atwood, *Organometallics,* 1985, **4**, 1162.

4   R. B. Jordan, *Reaction Mechanisms of Inorganic and Organometallic Systems*, 2nd edition, Oxford University Press, New York, 1998.

5   R. van Eldik, *Coord. Chem. Rev.,* 1999, **182***,* 373.

6   (a) A. Sargent, M. Hall and M. J. Guest, *J. Am. Chem. Soc.,* 1992, **114**, 517; (b) A. Sargent and M. Hall, *Inorg. Chem.*, 1992, **31**, 317.

7   S. J. P'Pool, M. A. Klingshirn, R. D. Rogers and K. H. Shaughnessy, *J. Organomet. Chem.,* 2005, **690**, 3522.

8   (a) F. Abu-Hasanayn, K. Krogh-Jespersen and A. S. Goldman*, J. Am. Chem. Soc.*, 1993, **115**, 8019; (b) F. Abu-Hasanayn, A. S. Goldman and K. Krogh-Jespersen, *Inorg. Chem.,* 1994, **33**, 5122.

9   K. Krogh-Jespersen, M. Czerw, K. M. Zhu, B. Singh, M. Kanzelberger, N. Darji, P. D. Achord, K. B. Renkema and A. S. Goldman, *J. Am. Chem. Soc.*, 2002, **124**,10797.

10 S. Sakaki, Y. Ujino and M. Sugimoto, *Bull. Chem. Soc. Japan*, 1996, **69**, 3047.

11 K. Fagnou and M. Lautens, *Angew. Chem. Int. Ed. Engl.*, 2002, **41**, 26.

12 See for example: (a) J. Burgess and C. D. Hubbard*, Adv. Inorg. Chem.*, 2003, **54**, 71; (b) R. van Eldik and C. D. Hubbard, *Adv. Phys. Org. Chem.,* 2006, **41**, 1; (c) J. P. Collman, L. S. Hegedus, J. R. Norton and R. G. Finke, *Principles and Applications of Organotransition Metal Chemistry*, 2nd ed., University Science Books, Mill Valley, California, 1987; (d) R. H. Crabtree, *The Organometallic Chemistry of the Transition Metals*, 3rd ed., Wiley, New York, 2001.

13 A. J. Downs and T. M. Greene, *Adv. Inorg. Chem.*, 1998, **46**, 101.

14 See for example: G. L. Geoffroy, G.S. Hammond and H.B. Gray, *J. Am. Chem. Soc.*, 1975, **97**, 3933.

15 (a) D. A. Wink and P.C. Ford, *J. Am. Chem. Soc.,* 1985, **107**, 5566; (b) D. A. Wink, P.C. Ford, *J. Am. Chem. Soc.*, 1987, **109**, 436.

16 (a) J. S. Bridgewater, B. Lee, S. Bernhard, J.R. Schoonover and P.C. Ford, *Organometallics*, 1997, **16**, 5592; (b) J. S. Bridgewater, T. L. Netzel, J. R. Schoonover, S. M. Massick, P. C. Ford, *Inorg. Chem.*, 2001, **40**, 1466.

17 T. E. Bitterwolf, W. B. Scallorn, J. T. Bays, C. A. Weiss, J. C. Linehan, J. Franz and R. Poli, *J.Organomet. Chem*., 2002, **652**, 95.

18 R. H. Schultz, *J. Organomet. Chem.*, 2003, **688**, 1.

19 (a) Y. Jean and A. Lledós, *Nouv. J. Chim*., 1986, **10**, 635; (b) S. Q. Niu and M. B. Hall, *Chem. Rev.,* 2000, **100**, 353.

20 .(a) F. Abu-Hasanayn, A. S. Goldman and K. Krogh-Jespersen, *J. Phys. Chem.,* 1993, **97**, 5890; (b) F. Abu-Hasanayn, K. Krogh-Jespersen and A. S. Goldman, *Inorg. Chem.*, 1993, **32**, 495; (c) F. Abu-Hasanayn, T. J. Emge, J. A. Maguire, K. Krogh-Jespersen and A. S. Goldman, *Organometallics*, 1994, **13**, 5177.

21 L. Vaska, *Acc. Chem. Res*., 1968, **1**, 335.

22 D. P. Paterniti and J. D. Atwood, *Polyhedron*, 1998, **17**, 1177.

23 Y. Zhao, N. E. Schultz, and D. G. Truhlar, *J. Chem. Theory and Comput,* 2006, **2,** 364.

24 M. J. Frisch, G. W. Trucks, H. B. Schlegel, G. E. Scuseria, M. A. Robb, J. R. Cheeseman, G. Scalmani, V. Barone, B. Mennucci, G. A. Petersson, H. Nakatsuji, M. Caricato, X. Li, H. P. Hratchian, A. F. Izmaylov, J. Bloino, G. Zheng, J. L. Sonnenberg, M. Hada, M. Ehara, K. Toyota, R. Fukuda, J. Hasegawa, M. Ishida, T. Nakajima, Y. Honda, O. Kitao, H. Nakai, T. Vreven, J. A. Montgomery Jr., J. E. Peralta, F. Ogliaro, M. Bearpark, J. J. Heyd, E. Brothers, K. N. Kudin, V. N. Staroverov, R. Kobayashi, J. Normand, K. Raghavachari, A. Rendell, J. C. Burant, S. S. Iyengar, J. Tomasi, M. Cossi, N. Rega, J. M. Millam, M. Klene, J. E. Knox, J. B. Cross, V. Bakken, C. Adamo, J. Jaramillo, R. Gomperts, R. E. Stratmann, O. Yazyev, A. J. Austin, R. Cammi, C. Pomelli, J. W. Ochterski, R. L. Martin, K. Morokuma, V. G. Zakrzewski, G. A. Voth, P. Salvador, J. J. Dannenberg, S. Dapprich, A. D. Daniels, Ö. Farkas, J. B. Foresman, J. V. Ortiz, J. Cioslowski, D. J. Fox, Gaussian 09 Revision D.01, Gaussian, Inc: Wallingford CT, 2013.

25 S. Grimme, J. Antony, S. Ehrlich and H. Krieg, *J. Chem. Phys*, 2010, **132**, 154104.

26 A. V. Marenich, C. J. Cramer, and D. G. Truhlar, *J. Phys. Chem. B*, 2009, **113**, 6378.

27 (a) K. K. Irikura and D. J. Frurip, *ACS Symposium Series*, 1998, **677**, American Chemical Society (ed), Washington, DC, 1998. (b) K. K. Irikura, *National Institute of Standards and Technology*, 2002.

28 M. V. Hopffgarten and G. Frenking, *Comput Mol Sci*, 2011, **2**,

29 G. te Velde, F.M. Bickelhaupt, E.J. Baerends, C.F. Guerra, S.J.A. Van Gisbergen, J.G. Snijders and T. Ziegler, *J. Comput. Chem.* 2001, **22**, 931.

30 E. van Lenthe, E. J. Baerends and J.G. Snijders, *J. Chem. Phys.*, 1993, **99**, 4597.

31 C. J. Huber, T. C. Anglin, B. H. Jones, N. Muthu, C. J. Cramer and A. M. Massari, *J. Phys. Chem. A*, 2012, **116**, 9279.

32 B. H. Jones and A. M. Massari, *J. Phys. Chem. B*, 2013, **117**, 15741.

33 (a) P. Pyykkö, S. Riedel and M. Patzschke, *Chem. Eur. J.*, 2005, **11**, 3511; (b) P. Pyykkö and M. Atsumi, *Chem. Eur. J.*, 2009, **15**, 186; (c) P. Pyykkö and M. Atsumi, *Chem. Eur. J.*, 2009, **15**, 12770.

34 B. Cordero, V. Gómez, A. E. Platero-Prats, M. Revés, J. Echeverría, E. Cremades, F. Barragán and S. Alvarez, *Dalton Trans.*, 2008, 2832.

35 Merino, V. I. Bakhmutov, and A. Vela, *J. Phys. Chem. A*, 2002, **106**, 8491.

36 M, Buhl, T. Steinke, P, Schleyer and R. Boese, *Angew. Chem. Int. Ed. Engl*., 1991, **30**, 1160.

37 G. L. Moxham, T. M. Douglas, S. K. Brayshaw, G. Kociak-Köhn, J. P. Lowe and A. S. Weller, *Dalton Trans.* 2006, 5492.

38 P. Paredes, J. Diez and M. P. Gamasa, *Organometallics*, 2008, **27**, 2597.

Please do not adjust margins **RSC Advances**

39 (a) M. Brookhart and M. L. H. Green, *J. Organomet. Chem.*, 1983, **250**, 395; (b) M. Brookhart, M. L. H. Green and G. Parkin, *P. N. A. S.*, 2007, **104**, 6908.
40 M. D. Fryzuk, L. Huang, N. T. McManus, P. Paglia, S. J. Rettig and G. S. White, *Organometallics*, 1992, **11**, 2979.
41 S. P. Green, C. Jones, D. P. Mills and A. Stasch, *Organometallics*, 2007, **26**, 3424.
42 M. A. Iron, J. M. L. Martin and M. E. van der Boom, *J. Am. Chem. Soc.,* 2003, **125**, 11702.
43 See for example: (a) M. Batool, T. A. Martin, A. G. Algarra, M. W. George, S. A. Macgregor, M. F. Mahon and M. K. Whittlesey, *Organometallics*, 2012, **31**, 4971. (b) M. Batool, T. A. Martin, M. Abu Naser, M. W. George, S. A. MacGregor, M. F. Mahon and M. K. Whittlesey, *Chem. Commun.,* 2011, **47**, 11225. (c) F. Hasanayn, P. Achord, P. Braunstein, H. J. Magnier, K. Krogh-Jespersen and A. S. Goldman, *Organometallics*, 2012, **31**, 4680. (d) M. Montag, I. Efremenko, Y. Diskin-Posner, Y. Ben-David, J. M. L. Martin and D. Milstein, *Organometallics,* 2012, **31**, 505.
44 S. A. Macgregor and P. Vadivelu, *Organometallics*, 2007, **26**, 3651.
45 $GaMe_3$ gas phase structure: (a) B. Beagley, D. G. Schmidling, and I. A. Steer, *J. Mol. Struct.* 1974, **21**, 437; $GaMe_3$ X-ray diffraction structure: (b) N. W. Mitzel, C. Lustig, R. J. F. Berger, N. Runebig, *Angew. Chem. Int. Ed.*, 2002, **41**, 2519; general discussion including other triorganogallium compounds: (c) G. H. Robinson, Gallium: Organometallic Chemistry in *The Encyclopedia of Inorganic Chemistry*, John Wiley and Sons. Ltd, 2006; (d) J. F. Malone and W. S. McDonald, *J. Chem. Soc. A*, 1970, 3362.
46 (a) C. Lustig and N. W. Mitzel, *Z. Natur. B: Chem. Sci.*, 2004, **59**, 140; (b) J.-C. Maire, U. Krüerke, M. Mirbach, W. Petz and C. Siebert, *Organogallium Halides*, Springer, Berlin Heidelberg, 1986; (c) K. K. Banger and A. F. Hepp, Gallium: Inorganic Chemistry in *The Encyclopedia of Inorganic Chemistry*, John Wiley and Sons. Ltd, 2006.

Please do not adjust margins

81x41mm (300 x 300 DPI)